Significant Reduction of Multipactor Effect in a Rectangular Waveguide with Periodically Grooved Metallic Surfaces

Ángela Coves [(1)], Sarah Maria Kira Bonte[(1)], Aitor Morales[(1)], J. Joaquín Vague [(2)], Vicente E. Boria [(2)], Isabel Montero[(3)]

[(1)] University Miguel Hernández of Elche. Avenida de la Universidad s/n, 03202 Elche, Alicante, Spain
Email: angela.coves@umh.es, sbonte@umh.es, aitor.morales@umh.es

[(2)] Universitat Politècnica de València. Camino de Vera s/n, E-46022, Valencia, Spain
Email: jvague@dcom.upv.es, vboria@upvnet.upv.es

[(3)] Instituto de Ciencia de Materiales de Madrid, CSIC, C/Sor Juana Inés de la Cruz 3, 28049, Madrid, Spain
Email: imontero@icmm.csic.es

INTRODUCTION

One of the main goals that microwave space components' designers strive to, is the ability of the devices to withstand the increasingly higher radiofrequency (RF) power requirements that must be considered at the output stages of transmitters. Nevertheless, these designs might suffer from the multipactor effect. Multipactor can be present in a wide variety of scenarios, such as satellite communication payloads or particle accelerators, for instance. This undesired effect occurs due to an avalanche of electrons in the component under vacuum conditions with high power and high frequency signals. This avalanche produces a resonant discharge inside the component with many possible harmful consequences. Among them, we can mention noise increase, signal degradation due to noise, local thermal heating, damage on the surface area where it occurs, and even the physical damage of the component, all of which finally lead to a limitation of the power level for satellite operations. Thus, in the last decades, the microwave space components' designers have focused their attention on the study of multipactor effect in the scenario of RF systems for space applications. This has been done in several types of microwave waveguides with different geometries, including empty waveguides [1-6], and also partially dielectric-loaded waveguides [7-12], although less work has been devoted to the avoidance (or reduction) of such effect.

Traditionally, two possible solutions have been addressed to minimize an electron discharge, and by that the damage it may cause. The first one is based on the use of material coatings or micro-porous surfaces with low secondary emission yield, obtaining an increase in the multipactor power threshold level of the component. These surface coatings reduce the multipactor effect, but their lifetime need to be demonstrated to be an optimum solution for space applications [13, 14]. Furthermore, the effect of an irregular micro-porous surface depends on the details of the manufacturing process and may yield to unacceptable variations from one piece to the other [15]. The second possible solution is to design the waveguide component in such a way that its electromagnetic field distribution may prevent the discharge. This can be done either avoiding regions of high field intensity and/or small gaps, or modifying the waveguide cross-section, like in [16], where a wedge-shaped hollow waveguide (instead of a conventional rectangular one) proved to deviate the resonant paths of the electrons toward regions with lower voltages. In this way, the probability of multipactor threshold for a certain input power level is reduced. However, the use of non-standard waveguides makes it necessary the design of expensive and bulky waveguide transformers.

Alternatively, as we will show, different profiles of 1-D or 2-D periodic grooved surfaces in the rectangular waveguide (RW) may lead to the increase of its multipactor power threshold level [17]. In this work, we propose a periodically grooved metallic surface profile on the waveguide walls of a RW to reduce the occurrence of multipactor effect under vacuum conditions. This profile has been applied to both, the top and bottom surfaces of the RW, showing a significant increase of the multipactor power threshold level compared to the same waveguide with smooth surfaces.

The reason why the resonant multipactor effect between the top and bottom grooved waveguide walls is reduced, differs from classical solutions based on the use of material coatings with low secondary emission yield. In the proposed rectangular waveguide with periodically grooved surfaces, the significant reduction of the multipactor effect achieved is caused by the decrease of the electromagnetic field intensity near the periodic grooves. Consequently, the electron staid time and the temporal dispersion of the secondary electron generation are increased. In this way, the generated secondary electrons are deviated from the resonant phase associated with the double-surface resonant multipactor effect.

ANALYSIS OF THE MULTIPACTOR EFFECT IN A RECTANGULAR WAVEGUIDE WITH SMOOTH SURFACES

As mentioned in the introduction, a comparative study has been performed of the power level at which the mutipactor breakdown occurs. To do so, we first analyse the effect in a nonstandard aluminium RW of width a = 22.86 mm, height b = 0.4 mm (a reduced height in order to lower the power threshold values to measurable ones), and length l = 18 mm, in which no changes regarding the metal surfaces are made. The electromagnetic fields in all the analyzed waveguides have been obtained with the full-wave electromagnetic (EM) analysis tool HFSS (v.2022.R2, Ansys), while the software tool used to study the multipactor effect in the RWs is SPARK3D (v2022, Dassault Systems), which first imports the EM fields inside the RW (previously computed with HFSS in this case), and then tracks the resulting electron motion by solving the 3-D Lorentz force equation, given the complex waveguide surfaces considered in next Section. The initial RW with smooth surfaces design is called 'Case A' in this paper.

In Fig. 1, the electric field intensity in the XY-plane is shown inside the waveguide, with a maximum of approximately $1.6 \cdot 10^4$ V/m in the centre of the waveguide.

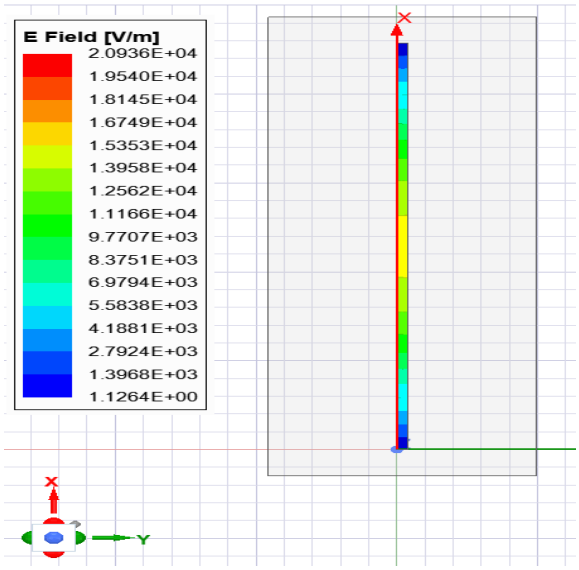

Fig. 1. Electric field intensity in the cross section of the RW with smooth surfaces (case A).

DESCRIPTION OF THE PROPOSED SURFACE PROFILE FOR THE REDUCTION OF THE MULTIPACTOR EFFECT

As already mentioned, this paper proposes to apply periodic grooves on the inner waveguide surfaces to avoid or reduce the possibility of an electron discharge. In particular, the grooves consist of a regular three-dimensional (3-D) triangular surface profile as shown in Fig. 2, whose base has been fixed to s = 50 µm (given that it must be small compared to the waveguide height so it slightly modifies the field distribution), and different depths t (see Fig. 2) have been considered. In all cases, a small chamfer of 3 µm on the peaks and on the valleys has been considered to take into account a practical implementation. The 3-D electric field distribution inside the proposed waveguide with metallic grooved surfaces has been calculated for different groove depths along either the longitudinal or transversal propagation direction, in order to search for an optimum configuration for reducing the multipactor effect. In all cases, we have checked that a good matching is achieved when connecting the proposed waveguides with periodically grooved metallic surfaces to waveguide ports with the same dimensions and smooth surfaces, which means that the proposed surface profile does not significantly modify the electrical response of the smooth waveguide. It must be said that a standard height RW will be even less affected by the surface corrugations. For comparison purposes, we have considered four different designs of RW with top and bottom grooved surfaces, which have been named as cases B, C, D and E, as detailed in Table 1.

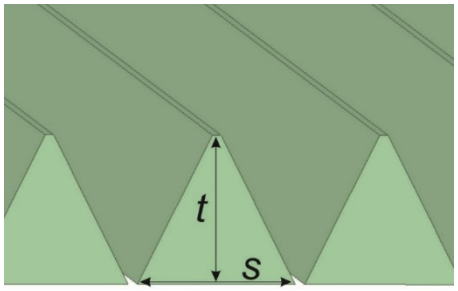

Fig. 2. Proposed grooves consisting of a three-dimensional (3-D) triangular surface profile with base *s* and depth *t*.

Table 1. Details of the different waveguide designs considered in the present study.

NO CORRUGATIONS	LOGITUDINAL CORRUGATIONS		TRANSVERSAL CORRUGATIONS	
CASE A	CASE B	CASE C	CASE D	CASE E
	t = 25 μm	t = 50 μm	t = 25 μm	t = 50 μm

Case B: RW with longitudinal grooves of t = 25 μm.

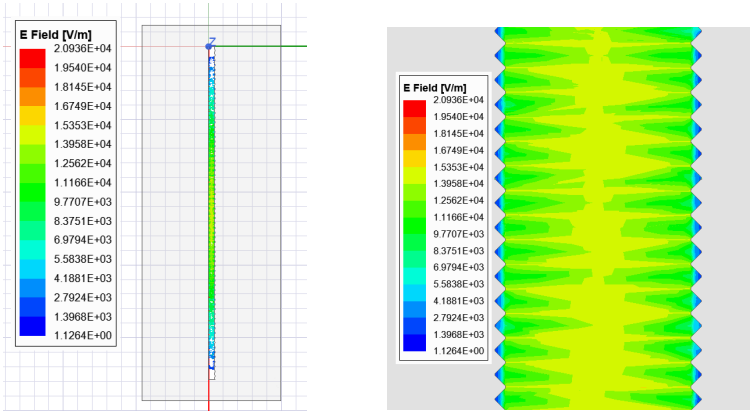

Fig. 3. Electric field intensity in the cross section of the RW with longitudinal grooves of t = 25 μm along the direction of propagation (case B).

Case C: RW with longitudinal grooves of t = 50 μm.

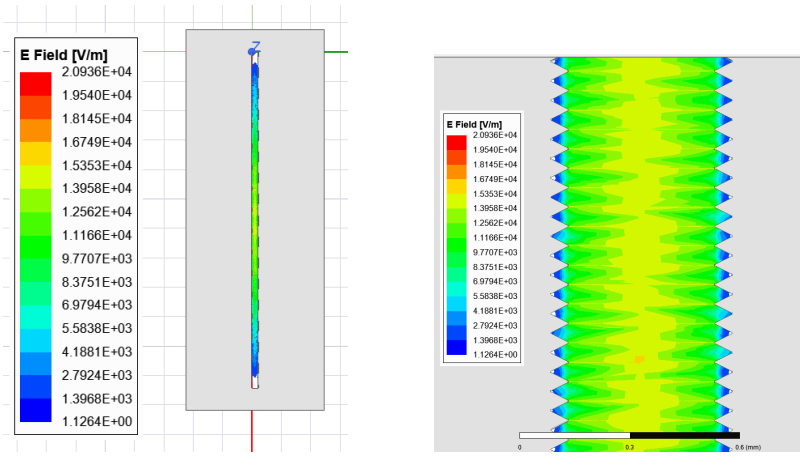

Fig. 4. Electric field intensity in the cross section of the RW with longitudinal grooves of t =50 μm along the direction of propagation (case C).

Case D: RW with transversal grooves of t = 25 μm.

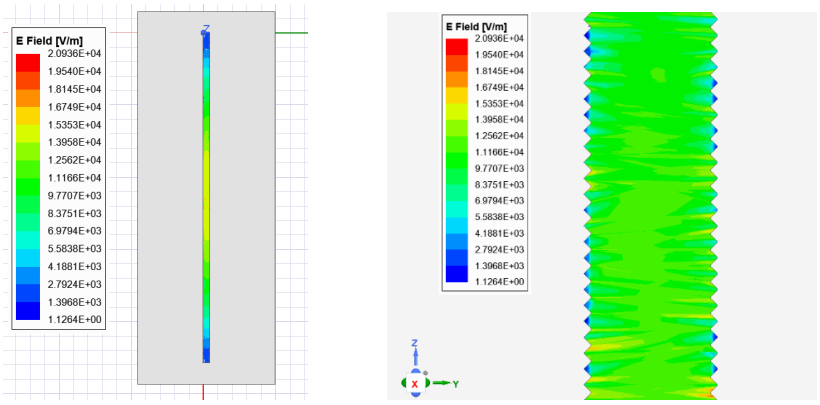

Fig. 5. Electric field intensity in the cross section of the RW with transversal grooves of t =25 μm along the direction of propagation (case D).

Case E: RW with transversal grooves of t = 50 μm.

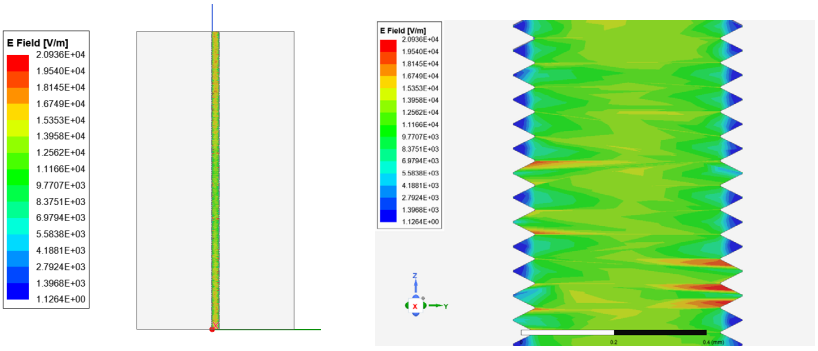

Fig. 6. (a) Electric field intensity in the cross section of the RW with transversal grooves of t =50 μm along the direction of propagation (case E).

Figs. 3-6 reveal that when performing grooves in the top and bottom waveguide surfaces, the otherwise uniform E-field distribution of the TE_{10} fundamental mode of the RW with smooth walls is substantially reduced near the top and bottom grooved waveguide walls. This reduction of the electric field at the waveguide walls is more accentuated for deeper grooves (i.e., for t = 50 μm), which will result in an increase of the multipactor power threshold, as we will see next. The following step is to analyze the multipactor power threshold in each one of these designs in order to find the best configuration.

STUDY OF THE MULTIPACTOR EFFECT IN A RECTANGULAR WAVEGUIDE WITH PERIODICALLY GROOVED METALIC SURFACES

Figs. 3-6 reveal a significant reduction of the electric field intensity inside the triangular corrugations with respect to case A (smooth surfaces), in which the TE_{10} electric field is uniform with the Y coordinate. Keeping in mind that multipactor is highly dependent on the electric field intensity in the regions where the secondary electrons are emitted, we can expect that a multipactor power threshold increase occurs. So, we can guess that the best results will be obtained with the design with the longitudinal corrugations and a depth of t = 50 μm (Case C).

Next, the multipactor effect is analysed in each one of the proposed designs with SPARK3D. In order to perform all the accurate multipactor simulations included in this article with SPARK3D, a homogeneous electron seeding has been defined inside the waveguide under study, and a number of 300 initial electrons have been considered. As SPARK3D is a simulation program, we repeated every analysis five times and then calculated the mean value of multipactor power

threshold, to obtain a final result that will be used to compare the proposed structures. The multipactor effect has been studied at the frequencies of 10 GHz, 11 GHz and 12 GHz.

In Table 2 the mean results for each design at the three studied frequencies can be seen, along with the increase in dB with respect to the waveguide with smooth surfaces. Next, Fig. 7 shows the multipactor power threshold of the transversal and longitudinal groove designs.

Table 2. Mean power threshold results for the multipactor analysis of the designs at 10 GHz, 11GHz and 12 GHz.

		NO CORRUGATIONS		LOGITUDINAL CORRUGATIONS				TRANSVERSAL CORRUGATIONS			
		CASE A		CASE B		CASE C		CASE D		CASE E	
				t = 0.025 mm		t = 0.050 mm		t = 0.025 mm		t = 0.025 mm	
	f	Power (W)	Order	Power (W)	Order	Power (W)	Order	Power (W)	Order	Power (W)	Order
	10 GHz	1251,54	4,06	2540,58	4,09	**4793,65**	2,5	2278,07	3,83	3543,61	1,8
Increase (dB) towards case A		---		3,07		**5,83**		2,60		4,52	
	11 GHz	1646,8	4,62	3218,6	4,57	**5912,17**	2,82	2906,08	4,13	4493,64	2,2
Increase (dB) towards case A		---		2,91		**5,55**		2,47		4,36	
	12 GHz	2128,07	5,18	4168,63	4,95	**7412,24**	2,97	3693,62	3,8	5568,46	1,92
Increase (dB) towards case A		---		2,92		**5,42**		2,39		4,18	

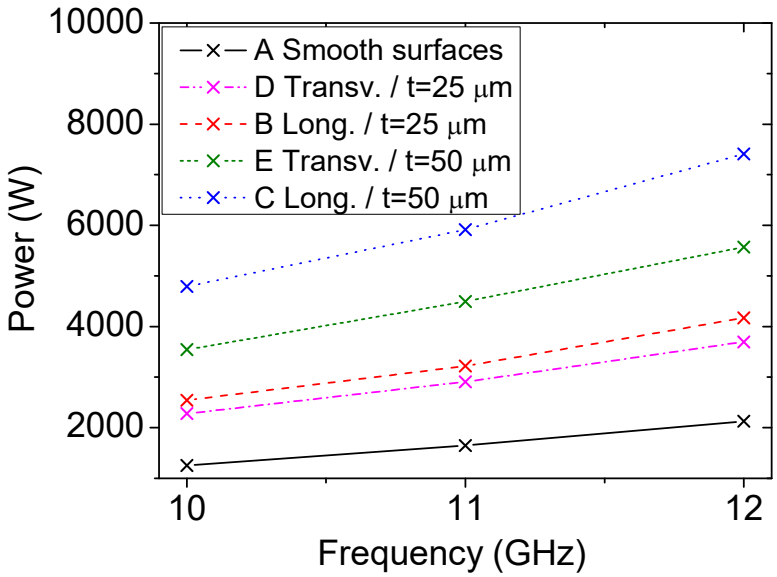

Fig. 7. Power threshold of the transversal and longitudinal groove designs at the different frequencies in dB.

In Table 2 it can be seen that in both cases, with transversal and longitudinal grooves, it is possible to improve multipactor with respect to the case without grooves. However, the improvement margins of the designs with the transversal corrugations are approximately 1 dB lower compared to longitudinal corrugations.. This means that, a priori, the transversal corrugations are less interesting than the longitudinal ones.

The table also shows that for all frequencies the design 'Case C' is the best one (see Table 2), looking at the power threshold at which the multipactor effect appears, because this case has the highest power threshold at all frequencies.

The greatest increase in the threshold power with respect to the threshold power of the smooth waveguide (case A) is for the frequency of 10 GHz. For this case, an increase of 5.83 dB is observed with respect to the power obtained for case A. For the waveguide with transversal grooves, the best result is obtained for the design 'Case E'. Once again, it corresponds to the design with the triangle depth of t = 50 μm and at the frequency of 10 GHz.

CONCLUSION

In this work, the goal was to reduce the multipactor effect by designing a surface profile that would decrease the electric field at the walls of the rectangular waveguide.

Indeed, the electric field was significantly decreased in the grooves near both walls of the waveguide, compared to that in the central region of the waveguide. To demonstrate the significant reduction in the expected multipactor effect, the power threshold in a rectangular waveguide with different depths of the grooved surfaces has been calculated, showing a significant increase in terms of the power handling capability of the waveguide with the proposed technique. Between the four possible considered designs, the optimal solution is obtained with the design of longitudinal corrugations and a depth of the periodic corrugations of t = 50 μm. In the future, this surface profile could be tried with other more complex microwave devices.

REFERENCES

[1] V. E. Semenov, E. I. Rakova, D. Anderson, M. Lisak, and J. Puech, "Multipactor in rectangular waveguides," Phys. Plasmas, vol. 14, no. 3, pp. 1–033501–033501-8, 2007.

[2] C. Vicente et al., "Multipactor breakdown prediction in rectangular waveguide based components," in IEEE MTT-S Int. Microw. Symp. Dig. Long Beach, CA, USA, Jun. 2005, pp. 1055–1058.

[3] A. M. Pérez, V. E. Boria, B. Gimeno, S. Anza, C. Vicente, and J. Gil, "Multipactor analysis in circular waveguides," J. Electromagn. Waves Appl., vol. 23, nos. 11–12, pp. 1575–1583, 2009.

[4] A. Frotanpour, B. G. Martinez, and S. Esfandiarpour, "Multipactor in dual-mode elliptical waveguide," in Proc. 31st Int. Rev. Prog. Appl. Comput. Electromagn. (ACES), Williamsburg, VA, USA, Mar. 2015, pp. 1–2.

[5] A. M. Pérez et al., "Prediction of multipactor breakdown thresholds in coaxial transmission lines for traveling, standing, and mixed waves," IEEE Trans. Plasma Sci., vol. 37, no. 10, pp. 2031–2040, Oct. 2009.

[6] J. J. Vague et al., "Study of the multipactor effect in groove gap waveguide technology," in IEEE Transactions on Microwave Theory and Techniques, vol. 70, no. 5, pp. 2566-2578, May 2022.

[7] G. Torregrosa, Á. Coves, C. P. Vicente, A. M. Pérez, B. Gimeno, and V. E. Boria, "Time evolution of an electron discharge in a parallel-plate dielectric-loaded waveguide," IEEE Electron Device Lett., vol. 27, no. 7, pp. 619–621, Jul. 2006.

[8] Á. Coves, G. Torregrosa-Penalva, C. Vicente, B. Gimeno, and V. E. Boria, "Multipactor discharges in parallel-plate dielectric-loaded waveguides including space-charge effects," IEEE Trans. Electron Devices, vol. 55, no. 9, pp. 2505–2511, Sep. 2008.

[9] E. Sorolla, M. Belhaj, J. Sombrin, and J. Puech, "New multipactor dynamics in presence of dielectrics," IEEE Trans. Plasma Sci., vol. 24, no. 10, Sep. 2017.

[10] G. Torregrosa, Á. Coves, B. G. Martinez, I. Montero, C. Vicente, and V. E. Boria, "Multipactor susceptibility charts of a parallel-plate dielectric-loaded waveguide," IEEE Trans. Electron Devices, vol. 57, no. 5, pp. 1160–1166, May 2010.

[11] A. Berenguer, Á. Coves, F. Mesa, E. Bronchalo, and B. Gimeno, "Analysis of multipactor effect in a partially dielectric-loaded rectangular waveguide," IEEE Trans. Plasma Sci., vol. 47, no. 1, pp. 259–265, Jan. 2019.

[12] A. Berenguer, Á. Coves, B. Gimeno, E. Bronchalo and V. E. Boria, "Experimental study of the multipactor effect in a partially dielectric-loaded rectangular waveguide," in IEEE Microwave and Wireless Components Letters, vol. 29, no. 9, pp. 595-597, Sept. 2019.

[13] I. Montero, L. Aguilera, D.Raboso and U. Wochner, "Antimultipactor Device", Patent WO2016042192A1, WIPO (PCT) , US10724141B2, CA2973088C, ES2564054B1, December 2016.

[14] R. L. Ives, C. Oldham, M. Gilmore and I. J. Kern, "Performance of multipactor coatings applied using atomic layer deposition," 2022 IEEE International Conference on Plasma Science (ICOPS), Seattle, WA, USA, 2022, pp. 1-1.

[15] Wan-Zhao Cui, Yun Li, Jing Yang, Tian-Cun Hu, Xin-Bo Wang, Rui Wang, Na Zhang, Hong-Tai Zhang, and Yong-Ning He, "An efficient multipaction suppression method in microwave components for space application", *Chinese Physics B*, Vol. 25, pp. 068401, 2016.

[16] J. Hueso, C. Vicente, B. Gimeno, V. E. Boria, S. Marini and M. Taroncher, "Multipactor effect analysis and design rules for wedge-shaped hollow waveguides," in IEEE Transactions on Electron Devices, vol. 57, no. 12, pp. 3508-3517, Dec. 2010.

[17] C.Chang, Y. D. Li, J. Verboncoeur, Y. S. Liu and C. L. Liu, "Suppressing double-metal-surface resonant multipactor by three dimensional wavy surface," *American Institute of Physics*, April 2017.